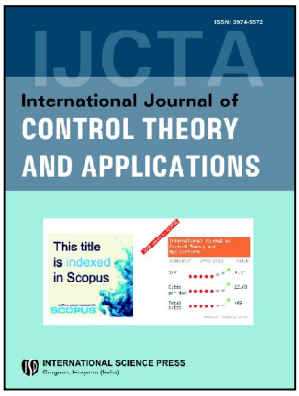

International Journal of Control Theory and Applications

ISSN : 0974-5572

Volume 10 • Number 6 • 2017

Laminar Fluid Flow and Heat Transfer Characteristics of Al_2O_3 Nanofluid in 180-degree Return Bend Pipe

Swetapadma Rout, Arnab Mukherjee, Ashok K. Barik and Prasanta K. Satapathy

Department of Mechanical Engineering, College of Engineering and Technology, Bhubnaeswar-751029, Odisha, India
E-mail-shwetapadma.rout@gmail.com; arnabapun@gmail.com; ashokbarik.mech@gmail.com; premdamayanti@yahoo.com

Abstract: Heat transfer and fluid flow characteristics for a laminar flow of Al_2O_3 nanofluid in a bend tube of triangular cross-section has been investigated numerically employing finite volume method. Governing equations for mass,momentum and energy have been solved iteratively in commercial software ANSYS Fluent 16. The duct Reynolds number, volume fraction of nanofluid, and aspect ratio have been varied from 200 to 2,000, 0 to 5%, and 0.866 to 6, respectively. Significant heat transfer enhancement has been observed when basefluid is replaced with nanofluid. Heat transfer enhancement with a high aspect ratio duct is found to be higher than a low aspect ratio duct. The performance evaluation criteria (PEC) decreases with the Reynolds number.

I. INTRODUCTION

Optimisation of geometry for engineering equipment with an aim to attain a higher thermal efficiency have been studied by many researchers [1-2]. Although geometrical modification enhances the heat transfer rate, the penalty for severe pressure drop may outweighs the benefits gained from geometrical modification. Thus, with an existing geometry, it is possible to augment heat transfer rate by replacing the conventional fluid with the water based nanofluids. Choi *et al.* [3] quantitatively studied some potential benefits of nanofluids for augmenting heat transfer rate by reducing the size, weight as well as the cost of thermal apparatuses. Heat transfer enhancement by nanofluids has been compressively studied by several researchers [4-6]. The increase in heat transfer surface area, heat capacity and thermal conductivity are important factors to enhance the heat transfer rate in nanofluids. Furthermore, it has been shown in Refs. [4-7] that the occurrence of inter-particle collisions help in intense mixing in the bulk fluid, which is responsible for an enhanced heat transfer rate. The convective heat transfer of CuO-water and Al_2O_3-water in a circular tube with constant wall temperature has been studied by Heris *et al.* [8]. An experimental study on convective heat transfer in developing region of circular tube has been carried out by Anoop *et al.* [9] using two different sizes of (150 nm and 45 nm) Al_2O_3 nanoparticles. The effect of Al_2O_3 particle volume fraction and its diameter on entropy generation has been studied numerically using finite volume method by Tabrizi and Seyfl [10]. The heat transfer rate was significantly enhanced with particle volume fraction and Reynolds number. Forced convection heat transfer for a developing laminar flow in a straight circular tube has been studied numerically by Bianco *et al.* [11]. The heat transfer performance of Al_2O_3 and CuO nanofluids in

the flat tubes of an automobile radiator have been studied numerically by Vajjha *et al.* [12]. A significant hike (i.e., 94%) in the heat transfer coefficient over the conventional fluid has been reported by them when 10% Al_2O_3 was added to water. Furthermore, Choi and Zhang [13] carried out a numerical investigation on heat transfer characteristics in bend pipe carrying Al_2O_3 nanofluid. It is clear from the above literature survey that a very few work has been carried out to study the heat transfer analysis for Al_2O_3-water nanofluid flowing in a triangular return bend pipe. So an attempt has been made to investigate the effects of volume fraction, Reynolds number and aspect ratio of a horizontally oriented triangular bend pipe on the heat transfer and fluid flow characteristics.

II. MATHEMATICAL MODELLING

2.1. Physical model and grid arrangement

The schematic diagram with applied boundary conditions for 180-degree bend pipes are shown in Fig. 1(a). The grid layout for the present computational domain along with the expended and cutaway view of the bend portion have shown in Fig. 1(b). The length of the pipe before and after the 180-degree bend are kept 20 times the hydraulic diameter of the pipe (D_h = 0.005 m) so as to ensure a fully developed laminar flow at the entrance of the bend section. A 180-degree bend tube with triangular cross section has been considered for the present analysis. The present pipe configuration along with the bend has been orientated horizontally. A constant radius of curvature has been taken for the investigation, although the hydraulic diameter of the duct is varied. Alumina-water (Al_2O_3-water) nanofluid is entered into the bend pipe at a uniform velocity of V_{in} and temperature of T_∞ = 300 K into the pipe through its inlet. A constant wall temperature of T_w / T_∞ = 1.21 has been applied to the bend walls. All the walls before and after the bend tube were maintained adaiabatic.

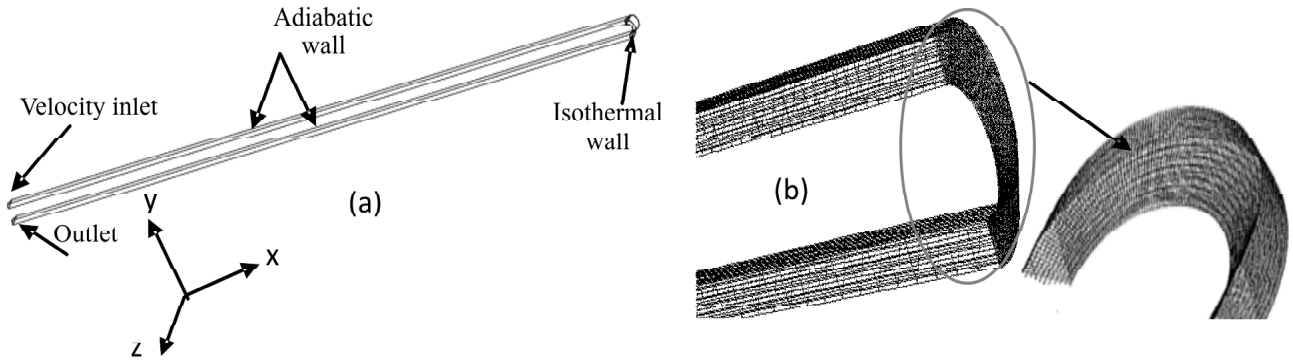

Figure 1: Schematic diagram of 180° bend pipe pipe with different boundary conditions(a) Grid arrangements for computational domain with enlarged view of the grid arrangement for bend portion of the pipe (b)

III. PHYSICAL PROPERTIES OF NANOFLUID

Since the nanoparticles are very small in diameter (37 nm), it is expected that these could be fluidized easily in the base fluid, and the resulting mixture may be considered as a homogenous single phase mixture. Thus, the thermo-physical properties of nanofluid are evaluated from some well-known classical formulae. Table 1 shows different thermo physical properties of nanoparticle and base fluid at temperature of 300 K and pressure of 1 bar.

The density (ρ_{nf}) [14-15], dynamic viscosity (μ_{nf}) [16-17], the specific heat (c_{nf}) [15-17], and the thermal conductivity of the mixture(i.e., Al_2O_3-water nanofluid) has been computed from the equations as given below:

Table 1
Thermo-physical properties of Al_2O_3nanoprticle and water

Properties	*Al_2O_3 nanoparticles (p)*	*Water (bf)*
Density, ρ (kg/m^3)	3880	998.2
Thermal conductivity, $k(W/m-K)$	36	0.597
Sp. heat, $c_p(J/kg-K)$	773	4182
Viscocity		9.93×10^{-4}

$$\rho_{nf} = (1-\phi)\rho_{bf} + \phi\rho_p \tag{1}$$

$$\frac{\mu_{nf}}{\mu_{bf}} = 123\phi^2 + 7.3\phi + 1 \tag{2}$$

$$c_{nf} = (1-\phi)c_{bf} + \phi c_p \tag{3}$$

$$\frac{k_{nf}}{k_{bf}} = 4.97\phi^2 + 2.72\phi + 1 \tag{4}$$

The duct Reynolds number, heat transfer coefficient and Nusselt number are computed as follows:

$$\mathrm{Re}_{Dh} = \rho_{nf} V_{in} D_h \Big/ \mu_{nf} \tag{5}$$

$$h = \frac{Q}{A(T_w - T_\infty)} \tag{6}$$

Here A is the area of the three walls of the tube in the bend region. Where constant temperature condition has been imposed, and Q is the sum of the heat of three walls. The Nusselt number is calculated as:

$Nu = \frac{hL}{k_{nf}}$, where L is the characteristics length.

IV. MATHEMATICAL FORMULATION

4.1. Governing differential equation

The conservation equations for mass, momentum and energy are discretized in a three-dimensional computational domain with refine grids in bend portion of the duct as shown in Fig. 1(a) and (b). In most of the practical applications, the size of the nanoparticles is usually kept below 100 nm. Thus, it is expected that these fine-sized particles mix thoroughly with the base fluid forming a homogenous mixture. This nature of the suspension validates the continuum approach. In conjunction with the arguments stated above, other assumptions considered for the present study are given as follows:

I. The flow in the bend pipe is considered as steady and laminar.

II. The slip velocity between nanoparticles and base fluid is negligible, and the thermal equilibrium between the continuous phase and discrete particles is prevailed.

III. The nanofluids are treated as incompressible and Newtonian with constant physical properties.

IV. The thermal radiation, viscous dissipation, and compression work are negligibly small in the energy equation. Thus, these are neglected in the energy equation.

The governing equations for conservation of mass, momentum and energy are written in vector form as follows:

Continuity equation: $$div(\rho_{nf} V) = 0 \tag{7}$$

Momentum equation: $$div(\rho_{nf} VV) = -gradP + \mu_{nf} \nabla^2 V \tag{8}$$

Energy equation: $$div(\rho_{nf} C_{p,nf} T) = div(k_{nf}\, gradT) \tag{9}$$

4.2. Boundary condition

Since governing equations are elliptic, nonlinear partial differential equations, the boundary conditions on all of its bounding surfaces are required. Thus, the velocity inlet boundary condition has been imposed at the tube inlet as nanofluid enters the domain with a uniform velocity V_{in} temperature T_{in} (which is equal to T_∞). At the pipe outlet, the outflow condition has been imposed. All the walls before and after the return bend are subjected to adiabatic boundary condition. The bend walls are only applied with the uniform temperature ($T_w / T_\infty = 1.21$). The mathematical descriptions of different boundary conditions used in the present study are given as follows:

$$\text{Pipe inlet: } v = w = 0, u = V_{in}, T = T_{in} = T_\infty \tag{10}$$

$$\text{Pipe outlet: } \frac{\partial \xi}{\partial n} = 0 \tag{11}$$

Where ξ represents any physical quantity in the computational domain, and n is the outward normal drawn to outlet of the pipe.

$$\text{Adiabatic walls of the pipe } u = v = w = 0, \frac{\partial T}{\partial x} = \frac{\partial T}{\partial y} = \frac{\partial T}{\partial z} = 0 \tag{12}$$

$$\text{Constant temperature bend walls } u = v = w = 0, \; T_x = T_y = T_z = T_w \tag{13}$$

4.3. Numerical solution procedure

The three-dimensional computational domain has been discretized using hexahedral cells. The discretized equations for mass, momentum, and energy are integrated over the control volume to yield a set of algebraic equations. The second order upwind scheme has been adopted for discretizing the convective and diffusion terms so as to maintain a better accuracy in the results. A staggered grid layout has been employed to compute the temperature and velocity components at centre of each control volume. SIMPLE algorithm [Patankar (18)] has been employed for pressure- velocity coupling to solve pressure correction equation. The set of algebraic equations are then solved iteratively using a point implicit (Gauss- Siedel) linear equation solver in conjunction with whole field residual method. The solution is declared conversed when the residuals(i.e, relative error) for momemtum and energy falls 10^{-4} and 10^{-7} respectively.

V. VALIDATION

Attempts have been made to validate the present numerical scheme with some of the existing data available in literature. It worth to mention here that there exits neither experimental nor numerical data to validate the heat

transfer from a return bend pipe of rectangular cross section carrying Al_2O_3-water nanofluid. As far as our knowledge is concerned, the numerical study on convective heat transfer in a return bend of circular cross section carrying Al_2O_3-water nanofluid by Choi and Zhang [13] was only available literature for the validation of our numerical results. Thus, the present results for axial velocity profiles are validated with the numerical results of Choi and Zhang [13] for a circular cross section return bend pipe. The dimensionless axial velocity profiles (U/U_{in}) have been plotted (i.e., Fig. 2.(a)) against the dimensionless axial distance (AA/D_h) drawn in the mid-plane of a return bend (180°) pipe. The mid-plane of 180° return bend with the line AA has been shown in Fig. 2.(b) for a better understanding of the velocity profiles.

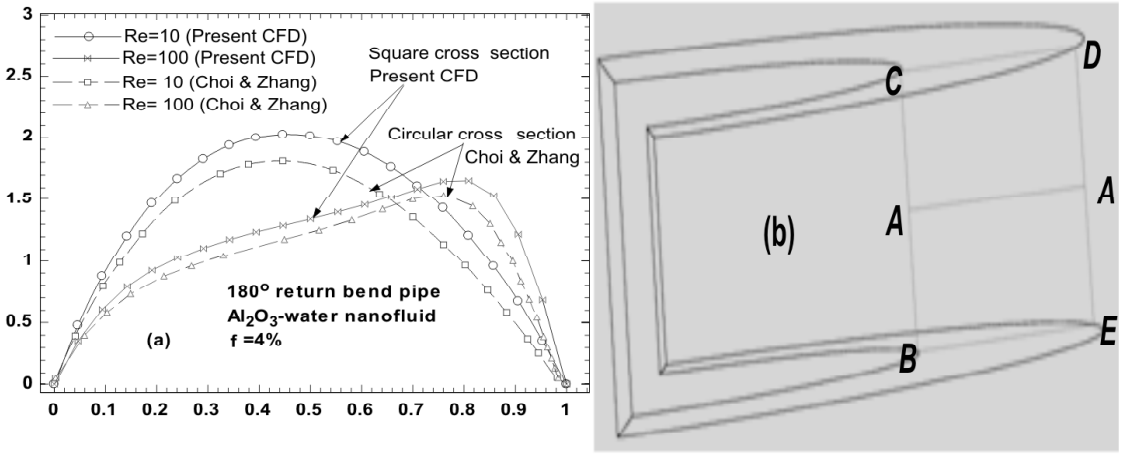

Figure 2: Variation of axial velocity along the line AA (a); position of the line AA in the 180° bend tube

It is quite evident from Fig. 2(a) that variation of velocity profiles along the line AA shows a similar trend that of the variation reported by Choi and Zhang [13]. At $Re_{Dh}=10$, the velocity profiles for both circular as well as rectangular pipes are approximately symmetric in shape. However, the symmetric nature of the velocity profiles are distorted at a higher Reynolds number ($Re_{Dh}=100$) showing a higher velocity towards the outer wall of the curved pipe. At higher Reynolds number, the higher tangential velocity enhances the centrifugal force at outer region of the curved pipe. As a result, the fluid flows at a higher velocity near this region. It is to be noted here that the present computed velocities are a little higher than the values given by Choi and Zhang[13]. This discrepancy in the results perhaps attributed to; (i) the cross section of the bend pipe, and (ii) the applied thermal boundary condition. In the present study, a curved pipe of rectangular ($AR=1$) cross section subjected to constant wall temperature has been employed; whereas a bend pipe of circular cross section with uniform wall heat flux was used Choi and Zhang[13].

VI. RESULTS AND DISCUSSIONS

6.1. Grid independent test

The grid sensitivity study has been carried out for the present simulation which shown in Fig.3. A triangular horizontal bend tube with aspect ratio=0.866 (aspect ratio is defined as the ratio of vertical height to horizontal side) carrying Al_2O_3-water nanofluid of volume fraction 4% has been considered for grid independent study. Initially, the computational domain is meshed with 8,000 cells, and then the subsequent grid refinement increases the cell size to 49500. It is observed that the average Nusselt number has been increased by 0.3966% as the number of cells is increased from 8,000 to 34500; and thereafter it increases by 0.0162% on increasing the

number of cells to 40,125. There after the Nusselt number nearly remains constant. Thus, the computational domain with 40,125 cells is considered as the grid independent domain for our futher analysis.

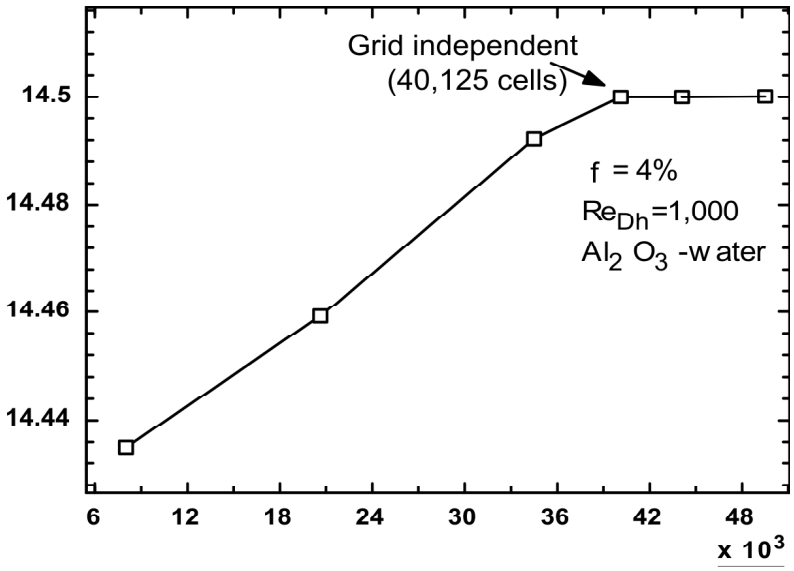

Figure 3: Variation of Nusselt number with number of cells

6.2. Effect of duct Reynolds number on heat transfer rate as a function volume fraction

The variation of average Nusselt number with Reynolds number at different volume fraction of the nanofluid in a triangular bend pipe is shown in Fig. 4(a). The Nusselt number is observed to increase with both Reynolds number and nanofluid volume fraction.

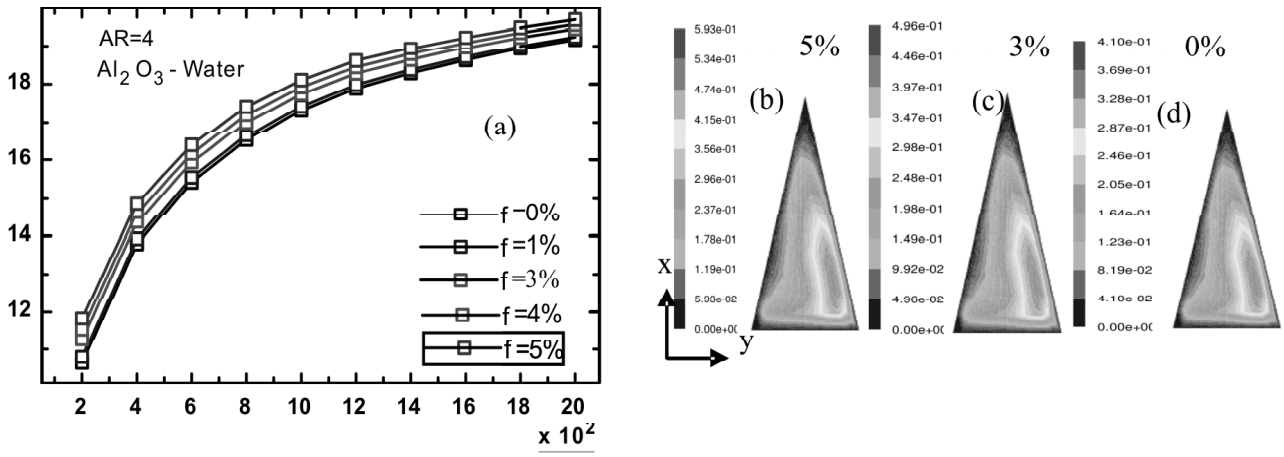

Figure 4: (a) Variation of Nusselt number with Reynolds number as function of nanofluid volume concentration and velocity magnitude contour at the mid-scction of bend tube in x-y plane (b) $\phi = 5\%$ **,(c)** $\phi = 3\%$ **, (d)** $\phi = 0\%$

This enhancement in heat transfer rate is attributed to the facts: firstly, the enhancement in thermal conductivity of mixture with the particle concentration, and secondly, the improvement in the fluid mixing leads to an increased energy transfer from the base fluid to the nanoparticles. Moreover, the Prandtl number of the nanofluid which depends on the nanofluid viscosity and thermal diffusivity is also increased with the volume fraction. It is evident from the velocity contour plot (i.e., Fig. 4(b) to (d), that the absolute velocity near the outer

wall of bend is higher than the inner wall which is because of the centrifugal force experienced by the flow while flowing through the bend. The z- velocity (i.e., w) and (i.e., v) y-velocity in x-y plane for three different volume fractions (ϕ = 5, 3, 0%) have been shown in Fig. 5 (a) to (f). The maximum value of w-component velocity at the outer duct wall for three different volume fractions (5, 3 and 0%) are 0.5 m/s, 0.4 m/s and 0.3 m/s, respectively. The maximum values of v-component velocities in x-y plane are 0.1 m/s, 0.08 m/s and 0.04 m/s, respectively for the above three volume fractions considered. The increased velocity with the volume fraction causes a strong convention heat transfer leading to an enhancement in the Nusselt number.

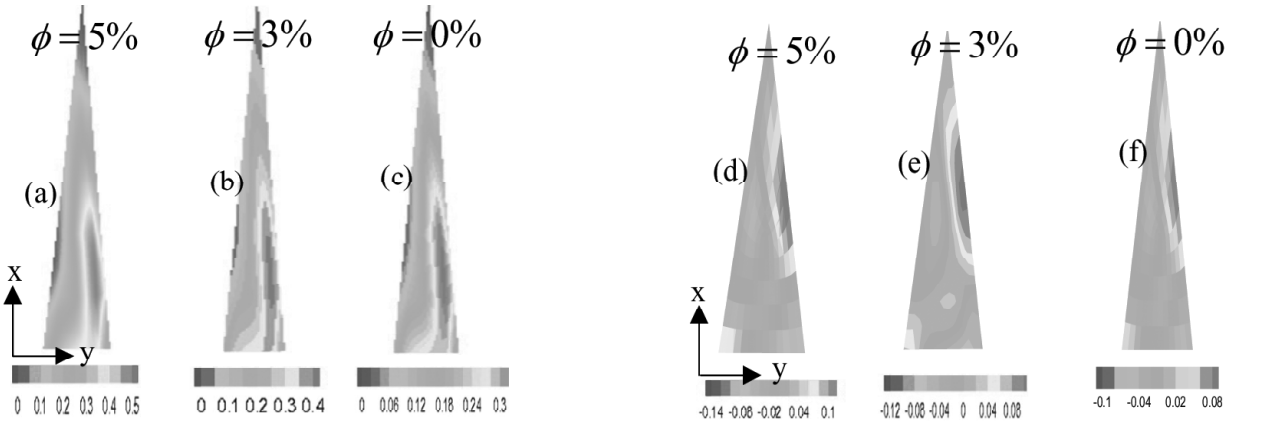

Figure 5: Velocity contour at the mid-scction of bend tube in x-y plane(w -velocity (a) $\phi = 5\%$,(b) $\phi = 3\%$,(c) $\phi = 0\%$) and (v -velocity (d) $\phi = 5\%$,(e) $\phi = 3\%$,(f) $\phi = 0\%$)

6.3. Effect of varying aspect ratio on heat transfer rate

Fig. 6(a) shows the effect of aspect ratio on the heat transfer characteristics for a triangular bend pipe carrying Al_2O_3-water nanofluid. As it can be seen, the Nusselt number has been increased with both Re_{Dh} and AR. At $\phi = 5\%$, for example, the Nusslet Number has been improved by 18.68 % and 28.11% ,respectively; when Reynolds number as well as the aspect ratio are changed from 8,00 to 2,000 and 0.86 to 4. For $\phi = 5\%$, two separate velocity contour plots in x-y plane passing through the mid-section of the bend with aspect ratio 0.866 and 6 have shown in Fig. 6 (b) and (c). A strong flow recirculation zone with higher velocity near the outer wall has been observed when a high aspect ratio duct is used. However, the recirculation zone is weakened in case of

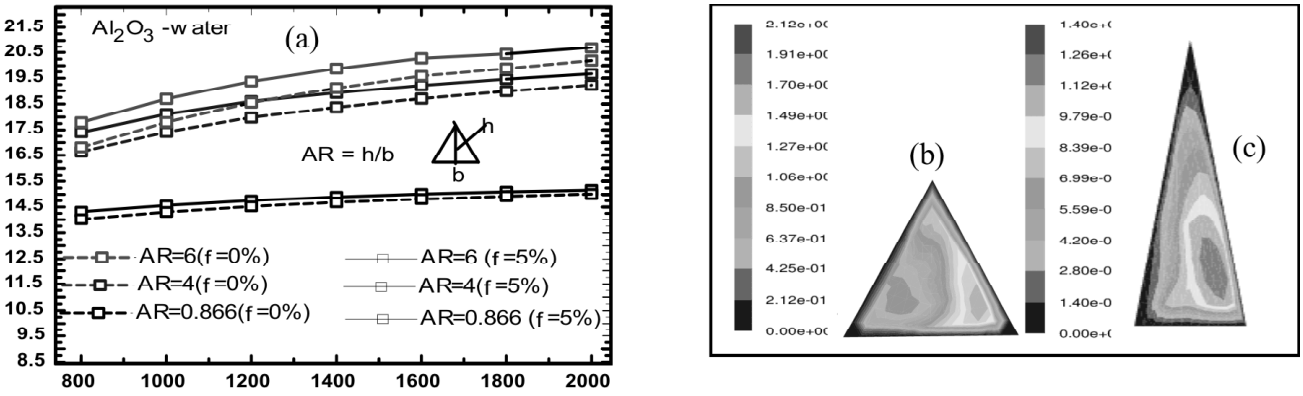

Figure 6: (a)Variation of Nusselt number with Reynolds number as function of duct aspect ratio (h/b) and velocity magnitude contour at the mid-scction of bend tube in x-y plane (b) AR =0.866 (c) AR = 6

a low aspect ratio duct. Thus, the heat transfer rate from the wall to bulk fluid is improved in high aspect ratio duct, so to enhance the Nusselt number.

6.4. Performance evaluation criteria (PEC)

The thermal performance of the nanofluid has been compared with that of the base fluid in terms of performance evaluation criteria (PEC). The performance evaluation criteria Roy *et al.* [19] has been defined as:

$PEC = \left| \frac{\dot{m} Cp_{nf} (T_{in} - T_{out})}{\forall \Delta p} \right|$. The PEC signifies the relative competition between the thermal energy and mechanical energy. The variation of PEC with duct Reynolds number has been shown in Fig.7 .It was observed that the PEC has been reduced with the duct Reynolds number. It is attributed to a higher pressure drop at a higher Reynolds number. The PEC of the nanofluids is seen to be lower than the water. Although the heat transfer enhancement is guaranteed with nanofluids, the pressure drop is significantly increases to overpower the benefits obtained from the heat transfer enhancement. Thus, the combined effect of thermal and mechanical energy lowers the PEC at high volume fraction. The lower value of PEC at high volume fraction has also been studied by Roy *et al.* [19].

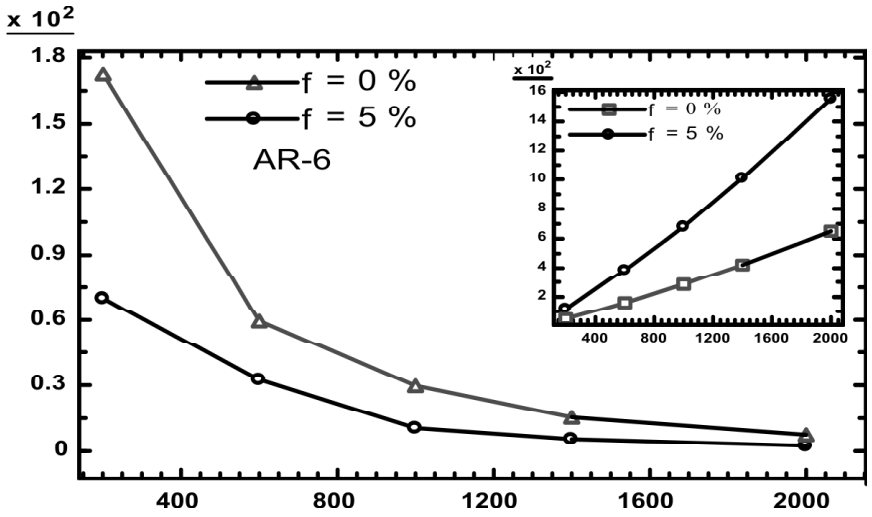

Figure 7: Variation of PEC with duct Reynolds number

VI. CONCLUSION

(a) The Nusselt number increases with the duct Reynolds number as well as the volume fraction of nano fluid.The higher heat transfer rate with ϕ ,is because of a higher absolute velocity near the outer wall of the curvature.

(b) It has been observed that the Nusselt number for an 180° bend pipe increases with the duct aspect ratio.

(c) The performance evaluation criterion (PEC) has been found to decrease with the Reynolds number.

REFERENCES

[1] Bejan A., Lorente S., Thermodynamic optimization of flow geometry in mechanical nad civil engineering, *Journal of Non-Equilibrium Thermodynamics*, Vol.26, (2001) pp. 305-354.

[2] Najafi H., Najafi B., Multi-objective optimization of a plate and frame heat exchanger via genetic algorithm, *Heat Mass Transfer* Vol. 46, (2000) pp. 639-647.

[3] Choi S.U.S., Zhang Z.G., Lookwood W. Yu, F. E., Grulke E.A., Anomalously thermal conductivity enhancement in nanotube suspension, *Applied Physics Letters* 79(14), (2001) pp. 2252-2254.

[4] Xuan Y., Li Q., Heat transfer enhancement with nanofluids, *International Journal of Heat and Fluid Flow*, Vol. 21, (2000) pp. 58-64.

[5] Wang X., Mujumdar A.S., Heat transfer characteristics of nanofluids: a review, *International Journal of Thermal Sciences*, Vol.46, (2007) pp.1-19.

[6] Kakaç S., Pramuanjaroenkij A., Review of convective heat transfer enhancement with nanofluids, *International Journal of Heat and Mass Transfer*, Vol.52, (2009) pp. 3187-3196.

[7] Barik, A. K., Rout, S. and Mukherjee, A., Numerical investigation on heat transfer enhancement from a protruded surface by cross-flow jet using Al_2O_3-water nanofluid, *International Journal of Heat and Mass Transfer,* Vol. (101), (2016) pp. 550-561.

[8] Heris S.Z., Esfahany M.N., Etemad S.G., Experimental investigation of convective heat transfer of Al2O3/water nanofluid in circular tube, *International Journal of Heat and Mass Transfer*,Vol. 28, (2007) pp. 203-210.

[9] Anoop K.B., Sunderrajan T., Das,S.K., Effect of particle size on convective heat transfer in nanofluids in developing region, *International Journal of Heat and Mass Transfer*,Vol. 52, (2009) pp. 2189-2195.

[10] Tabrizi A., Seyf H.R., Analysis of entropy generation and convective heat transfer of Al2O3 nanofluid flow in a tangential micro heat sink, *International Journal of Heat and Mass Transfer*, Vol.55, (2012) pp.4366-4375.

[11] Bianco V., Chiacchio F., Manca O., Nardini S., Numerical investigation of nanofluids forced convection in circular tubes, *Applied Thermal Engineering*, Vol.29, .(2009) pp. 3632-3642.

[12] Vajjha R.S., Das D.K., Namburu P.K. (2013), Numerical study of fluid dynamic and heat transfer performance of Al2O3 and CuO nanofluids in the flat tubes of a radiator, *International Journal of Heat and Fluid Flow*, Vol. 31, (2012) pp. 613-621.

[13] Choi j., Zhang Y., Numerical simulation of laminar forced convection heat transfer of Al_2O_3-water nanofluid in a pipe with return bend, *International Journal of Thermal Sciences*, Vol.55, (2009) pp. 90-102.

[14] Akbarinia A., Behzadmehr A., Numerical study of laminar mixed convection of nanofluid in horizontal curved tubes, *Applied Thermal Engineering*, Vol.27, (2007) pp. 1327-1337.

[15] Maiga S.E.B., Palm S.J., Nguyen C.T., RoyG., Galanis N., Heat transfer enhancement by using nanofluids in forced convection flows, *International Journal of Heat and Fluid Flow*, Vol.26, (2005)pp. 530-546.

[16] Wang X., Xu X., Choi S.U.S., Thermal conductivity of nanoparticle–fluid mixture, *Journal of Thermophysics and Heat Transfer* Vol.13, (1999) pp. 474–480.

[17] Pak B.C., Cho Y.I, Hydrodynamic and heat transfer study of dispersed fluids with submicron metallic oxide particles, *Experimental Heat Transfer*, 11(12), (1998) pp. 151-170.

[18] Patankar S.V., *Numerical Heat Transfer and Fluid Flow*, Hemisphere Publishing Corporation, New York, USA. (1980).

[19] G. Roy G, I. Gherasim, F. Nadeau, G. Poitras, C.T. Nguyen, Heat transfer performance and hydrodynamic behaviour of turbulent nanofluid radial flows. *International Journal of Thermal Sciences* 58 (2012) pp. 120-129.